

Do Low Levels of Metallicity Influence Cooling and Collapse of Ionized Gas in Small Protogalactic Halos?

A.-K. Jappsen¹, S. C. O. Glover^{1,2}, R. S. Klessen¹, M.-M. Mac Low²

¹*Astrophysikalisches Institut Potsdam,*

*An der Sternwarte 16, 14482 Potsdam, Germany; akjappsen@aip.de, sglover@aip.de,
rklessen@aip.de*

²*Department of Astrophysics, American Museum of Natural History,
79th Street at Central Park West, New York, NY 10024-5192, USA; mordecai@amnh.org*

ABSTRACT

We study the influence of low levels of metal enrichment on the cooling and collapse of ionized gas in small protogalactic halos using three-dimensional, smoothed particle hydrodynamics simulations. Our initial conditions represent protogalaxies forming within a fossil H II region – a previously ionized H II region which has not yet had time to cool and recombine. Prior to cosmological reionization, such regions should be relatively common, since the characteristic lifetime of the likely ionizing sources are significantly shorter than a Hubble time. We show that in these regions, H₂ is the dominant and most effective coolant, and that it is the amount of H₂ formed that controls whether or not the gas can collapse and form stars. For metallicities $Z \leq 10^{-3} Z_{\odot}$, metal line cooling alters the density and temperature evolution of the gas by less than 1% compared to the metal-free case at densities below 1 cm⁻³ and temperatures above 2000 K. However, at higher densities and lower temperatures metal line cooling does become more important, and may affect the ability of the gas to fragment. Finally, we find that an external ultraviolet background delays or suppresses the cooling and collapse of the gas regardless of whether or not it is metal-enriched.

Subject headings: galaxies: formation — molecular processes — stars: formation

1. Introduction

Within the framework of cold dark matter (CDM) cosmology the formation of structure proceeds in a hierarchical fashion. At high redshifts, low-mass halos with virial temperatures less than $\sim 10^4$ K are abundant. The cooling of primordial gas in these halos is regulated by

molecular hydrogen, as H_2 is the only coolant present in significant quantities that remains effective at temperatures below 10^4 K (Saslaw & Zipoy 1967; Peebles & Dicke 1968; Matsuda et al. 1969). Tegmark et al. (1997) developed analytic methods to model early baryonic collapse via H_2 cooling. Numerical studies of the formation of primordial gas clouds and the first stars indicate that this process likely began as early as $z \sim 30$ (Abel et al. 2002; Bromm et al. 2002). Yoshida et al. (2003) further utilized simulations to develop a semi-analytic model based on the Tegmark et al. (1997) methods and included the effects of dynamical heating caused by the thermalization of kinetic energy of infall into a deepening potential. Both approaches suggest that only gas in halos more massive than some critical mass M_{crit} will cool effectively. Much of this work has recently been reviewed by Bromm & Larson (2004), Ciardi & Ferrara (2005) and Glover (2005).

Population III stars are the first potential producers of UV photons that can contribute to the reionization process, and are the first producers of the metals required for the formation of population II stars. An important question is whether small protogalaxies that formed within the relic H II regions left by these first stars could form stars themselves, or whether the elevated temperatures and fractional ionizations found in these regions suppressed star formation until larger protogalaxies formed. In a recent analytical study, Oh & Haiman (2003) argue that the first stars injected sufficient entropy into the early intergalactic medium (IGM) by photoionization heating and supernova explosions to strongly suppress further star formation inside low-mass protogalactic halos in the affected regions. On the other hand, previous numerical work by Ricotti et al. (2002), as well as our own simulations of hot, ionized gas in small protogalactic halos show that gravitational collapse mediated by H_2 cooling remains possible in such regions, within protogalaxies with masses above a certain threshold, implying that in these systems star formation is not strongly suppressed.

A further form of negative feedback that must be taken into account comes from UV photons within the Lyman-Werner bands of H_2 , which are produced in large numbers by massive population III stars and which can photodissociate H_2 , thereby quenching molecular hydrogen cooling and delaying the cooling and collapse of the primordial gas (Haiman et al. 2000; Machacek et al. 2001; Glover & Brand 2001).

Metals produced by the first stars will also be injected into some fraction of the ionized volume, and so will be present in gas falling into new or existing protogalactic halos. The question then arises as to how this low level of metal enrichment affects the ability of the gas to cool and collapse. Bromm et al. (2001) studied the collapse of cold, metal-enriched gas, and argued that there exists a critical metallicity Z_{crit} below which the gas fails to undergo continued collapse and fragmentation. However, their simulations did not allow for H_2 formation and H_2 cooling, which is expected to play an important role unless the external

UV background is extremely strong. Also, by starting with cold gas they implicitly assume that no extra entropy or energy has been added to the gas during its enrichment, although as Oh & Haiman (2003) have shown this is unlikely to be the case. We re-examine this question using more appropriate initial conditions and a more detailed treatment of the cooling and chemistry of the metal-poor gas.

Here we present simulations showing that metals do not dominate the cooling of ionized gas in small protogalactic halos, and that the question of whether or not gas in a particular halo collapses is entirely determined by the amount of H₂ forming in that halo. We reach the same conclusion regardless of whether or not the gas is illuminated by a Lyman-Werner UV background, as in the absence of H₂ the metals themselves do not provide enough cooling to allow the gas to collapse.

2. Simulations

2.1. Numerical Method

To help us to assess the influence of metals on the cooling and collapse of gas in small protogalactic halos, we performed a number of numerical simulations. During collapse, gas increases in density by several orders of magnitude, and so is best simulated by a numerical method with a high dynamical range. We therefore chose smoothed particle hydrodynamics (SPH). Excellent overviews of the method, its numerical implementation, and some of its applications are given in reviews by Benz (1990) and Monaghan (1992). We use the parallel code GADGET, designed by Springel, Yoshida, & White (2001). SPH is a Lagrangian method for simulating astrophysical flows, in which the fluid is represented by an ensemble of particles, with flow quantities at a particular point obtained by averaging over an appropriate subset of neighboring SPH particles.

As we want to represent gas that has collapsed beyond the resolution limit of the simulation in a numerically robust manner, we have modified the code to allow it to create sink particles – massive, non-gaseous particles, designed to represent dense cores, that can accrete gas from their surroundings but otherwise interact only via gravity (Bate et al. 1995). The design and implementation of our sink particle algorithm is discussed in Jappsen et al. (2005).

2.2. Chemistry and Cooling

We have further modified GADGET to allow us to follow the non-equilibrium chemistry of the major coolants in both primordial and low metallicity gas. We track the non-equilibrium abundances of H_2 , H^+ , C^+ , O^+ and Si^+ . Using conservation laws for charge and element abundance we also follow the abundances of H , e^- , C , O and Si . The ions H^- and H_2^+ are also included in our chemical network, but because they reach equilibrium on very short time scales, we do not attempt to follow their abundances directly in our simulations. Instead, their abundances are computed only as required, under the assumption that they reach equilibrium instantaneously.

To compute the rate of photochemical reactions (such as the photodissociation of H_2) in runs in which an ultraviolet background is present, we assume a background spectrum that has the shape of a 10^5 K black-body (as should be typical of the brightest population III stars – see e.g. Cojazzi et al. 2000), cut off at energies greater than 13.6 eV to account for absorption by neutral hydrogen in the IGM. We quantify the strength of the background by fixing the flux at the Lyman limit: $J(\nu_\alpha) = 10^{-21} J_{21} \text{ erg s}^{-1} \text{ cm}^{-2} \text{ Hz}^{-1} \text{ sr}^{-1}$.

If sufficient H_2 forms within the protogalaxy, it will begin to self-shield, reducing the effective photodissociation rate. An exact treatment of the effects of self-shielding is computationally infeasible, as it would require us to solve for the full spatial, angular and frequency dependence of the radiation field at every timestep. Instead, we have chosen to incorporate it in an approximate manner. We assume that the dominant contribution to the self-shielding at a given point in the protogalaxy comes from gas close to that point, and so only include the contribution to the self-shielding that comes from nearby H_2 .

Finally, we assume that ionization from X-rays or cosmic rays is negligible. Previous work suggests that even if a low level of ionization from such sources is present, it will not have a major effect on the outcome of the collapse (Glover & Brand 2003; Machacek et al. 2003). In any case, the initial fractional ionization in our simulations is very much higher than could be produced by a realistic flux of X-rays or cosmic rays.

A second major modification that we have made to the GADGET code is a treatment of radiative heating and cooling. In primordial gas, we include cooling from three main sources: electron impact excitation of atomic hydrogen (Lyman- α cooling), which is effective only above about 8000 K, rotational and vibrational excitation of H_2 , and Compton cooling. Rates for Lyman- α cooling and Compton cooling were taken from Cen (1992), while for H_2 ro-vibrational cooling we used a cooling function from Le Bourlot et al. (1999). Additionally, in cases where the gas is metal enriched we compute the amount of fine structure cooling coming from C , C^+ , O , Si and Si^+ . In this calculation, we include the effect of excitation

of the fine structure lines by the CMB, which prevents the gas from cooling below T_{CMB} . We also include heating from H_2 photodissociation, following Black & Dalgarno (1977), and from the ultraviolet pumping of H_2 , following Burton et al. (1990).

We do not include cooling from HD, as this is only significant compared to H_2 at temperatures $T \ll 1000\text{K}$ which are not reached in our current simulations. Cooling from other primordial molecules and molecular ions (e.g. LiH, H_3^+) is likewise negligible at the densities and temperatures considered here. Heavy molecules such as CO are also omitted, as they form in significant abundances only at densities much greater than those considered in this paper. Finally, we do not include the effects of dust, as previous work has shown that it does not become a major coolant until very high densities are reached and that its contribution to the H_2 formation rate is negligible at densities $n < 100 \text{ cm}^{-3}$ (Omukai et al. 2005).

A more detailed discussion of our treatment of primordial chemistry and cooling is given in Glover et al. (2005), while the extensions that are required in order to allow us to model low metallicity gas are discussed in Jappsen et al. (2006).

2.3. Initial Conditions

In this paper we present the results of a first suite of simulations of protogalactic collapse (see Table 1). We initialize each of our simulations with gas that is hot ($T_g = 10^4 \text{ K}$) and fully ionized. The physical situation that these initial conditions are intended to represent is a protogalaxy forming within what Oh & Haiman (2003) term a fossil H II region – an H II region surrounding an ionizing source that has switched off, containing gas that has not yet had time to cool and recombine. Prior to cosmological reionization, such regions should be relatively common, since the characteristic lifetime of the likely ionizing sources – massive population III stars and/or active galactic nuclei – are significantly shorter than the Hubble time.

For our purposes, we do not need to follow the assembly history of the dark matter halo in which the protogalaxy resides, or to study the response of the dark matter halo to the cooling of the gas. Therefore, we choose to model the influence of the dark matter halo (hereafter simply the ‘halo’) by using a fixed background potential. To construct this potential, we assume that the halo is spherically symmetric, with the density profile of Navarro, Frenk, & White (1996):

$$\rho_{\text{dm}}(r) = \frac{\delta_c \rho_{\text{crit}}}{r/r_s(1+r/r_s)^2}, \quad (1)$$

where r_s is a scale radius, δ_c is a characteristic (dimensionless) density and $\rho_{\text{crit}} = 3H^2/8\pi G$ is the critical density for closure. Following Navarro et al. (1996) we calculate the characteristic density and the scale radius from a given redshift and dark halo mass. We truncate the halo at a radius r_t where ρ_{dm} equals the background density at this redshift. In all of the runs presented here, the halo mass is $7.8 \times 10^5 M_\odot$ and the redshift is $z = 25$. The virial temperature of the resulting halo is 1900 K. In physical units, the scale radius of the halo is 29 pc and the full computational volume is a box of side length 1 kpc. We use periodic boundary conditions for the hydrodynamic part of the force calculations to keep the gas bound within the computational volume. The self-gravity of the gas and the gravitational force exerted by the dark matter potential are not calculated periodically since we assume that other dark matter halos and their gas content are distant enough to neglect their gravitational influence.

We begin our simulations with a uniform distribution of gas with an initial density ρ_g , taken to be equal to the cosmological background density, and then allow the gas to relax isothermally until it reaches hydrostatic equilibrium. Note that this initial phase of the simulation is merely a convenient way to generate the appropriate initial conditions for the simulation proper, and so we do not include the effects of chemical evolution or cooling during this phase. The mass of gas present in our simulation was taken to be a fraction $\Omega_b/\Omega_{\text{dm}}$ of the total mass of dark matter, where the dark matter density $\Omega_{\text{dm}} = \Omega_m - \Omega_b$, and where Ω_b is the baryon density and Ω_m is the matter density. We take values for the cosmological parameters from Spergel et al. (2003) of $\Omega_b = 0.047$ and $\Omega_m = 0.29$, giving us a total gas mass of $M_g = 0.19 M_{\text{dm}}$. M_{dm} is the sum of the halo mass and the mass of the dark matter background in the simulated volume, and has a value $M_{\text{dm}} = 1.84 \times 10^6 M_\odot$. Therefore, $M_g = 3.5 \times 10^5 M_\odot$. We use 1.4×10^5 SPH particles to represent the gas, and so each particle has a mass $m_{\text{part}} = 2.5 M_\odot$. Our SPH smoothing kernel encompasses approximately 40 particles and since we need twice this number in order to properly resolve gravitationally bound objects (Bate & Burkert 1997), our mass resolution is therefore $M_{\text{res}} \simeq 80 m_{\text{part}} = 200 M_\odot$.

To prevent artificial fragmentation or other numerical artifacts from affecting our results, it is necessary either to halt the simulation before the local Jeans mass, M_J falls below M_{res} in any part of the simulation volume, or to use sink particles to represent regions where $M_J < M_{\text{res}}$. In the runs presented here we introduce sink particles with an accretion radius of 5 pc when the density rises above 500 cm^{-3} . At this density M_J exceeds M_{res} as long as $T > 30 \text{ K}$. As this is smaller than the CMB temperature at $z = 25$, and much smaller than the temperature reached by the gas in our simulations, we always satisfy the Bate & Burkert (1997) resolution criterion by a comfortable margin.

We follow the simulation for a Hubble time of ~ 100 Myr at a redshift of $z = 25$. After more than a Hubble time our assumption of an isolated dark matter halo will no longer be valid, since most halos will have undergone at least one major merger or interaction by this time. The dynamical time within the halo varies between 4 Myr in the center and 450 Myr in the outer regions.

We study both zero metallicity gas and gas that has been enriched to $10^{-3} Z_{\odot}$. A metallicity of $Z = 10^{-3} Z_{\odot}$ is an upper limit derived from QSO absorption-line studies of the low column density Lyman- α forest at $z \sim 3$ (Pettini 1999). Estimates of the globally-averaged metallicity produced by the sources responsible for reionization are also typically of the order of $10^{-3} Z_{\odot}$ (see e.g. Ricotti & Ostriker 2004).

In our simulations of metal-enriched gas, we assume that mixing is efficient and that the metals are spread out uniformly throughout the computational domain. We also assume that the relative abundances of the various metals in the enriched gas are the same as in solar metallicity gas; given the wide scatter in observational determinations and theoretical predictions of abundance ratios in very low metallicity gas (see the discussion in Glover 2006), this seems to us to be the most conservative assumption. However, variations in the relative abundances of an order of magnitude or less will not significantly alter our results. We have denoted runs with zero metallicity with “Z” and low metallicity with “L”.

We also investigate the influence of a UV background. By $z = 25$ a considerable UV background may already have developed (Haiman et al. 2000; Glover & Brand 2003). Indeed, if cosmological reionization is to occur somewhere in the redshift range 17 ± 5 , as is suggested by the WMAP polarization results (Kogut et al. 2003), there must already be a fairly strong background in place. To explore how the presence of a UV background will influence our conclusions, we have run several sets of simulations in which the strength of the UV background varies.

3. Results

3.1. Zero Metallicity Gas

Figures 1 and 2 compare the time evolution of the number density and temperature of the gas averaged over all SPH particles within the scale radius r_s for the runs with zero metallicity gas. After 50 Myr gas in the center of the halo in run Z1 starts to collapse rapidly. This is consistent with the finding by Yoshida et al. (2003) that gas in small protogalactic halos with a mass above $7 \times 10^5 M_{\odot}$ is able to cool efficiently via H₂ cooling. In run Z2, an imposed UV background of strength $J_{21} = 0.01$ photodissociates some of the molecular gas,

reducing the effectiveness of H₂ cooling and delaying collapse by more than 30 Myr compared to run Z1. A further increase in UV background by a factor of 10 completely inhibits the collapse of the gas within the time frame of our simulation. These results agree with the findings of Haiman et al. (2000), Machacek et al. (2001), and Mashchenko et al. (2005).

Table 1 gives the properties of the gas within the scale radius after 100 Myr of evolution. The table lists the minimum central temperature $T_{c,\min}$ and the maximum central density $n_{c,\max}$. We also calculate the fractional H₂ abundance with respect to the total number of hydrogen nuclei, and list the maximum central value, $x_{H_2,c,\max}$, in the table. The mass fraction of gas within a sink particle is denoted by f_{sink} . Because we have no information on the density and temperature distribution within the sink particle radius, we adopt the values at time of sink particle formation in Table 1. Note that as the gas in run Z3 does not collapse, it never reaches the density required for a sink particle to form.

The large fraction of the gas found within the sink particle at the end of run Z1 clearly shows the advanced state of the collapse, which is due to the effective cooling provided by the H₂. When a UV field is present, some of the H₂ is dissociated and so H₂ cooling is less effective. If the field strength is only $J_{21} = 0.01$, then this merely delays cooling and collapse, whereas a field strength of $J_{21} = 0.1$ is sufficient to prevent the gas from collapsing.

3.2. Metal-Enriched Gas

Next we compare the behaviour of gas with a metallicity $Z = 10^{-3} Z_{\odot}$ with that of primordial gas. In Figures 3 and 4 we show the time evolution of the relative differences between the central density and the central temperature in our two sets of runs. At times $t < 50$ Myr, the differences between the metal-enriched runs and the zero-metallicity runs are less than 1 %, and they remain below 10 % for the entire duration of the simulation.

Our results demonstrate that the cooling of the gas at densities below 1 cm⁻³ and temperatures above 2000 K is barely influenced by the presence of metals: fine structure cooling contributes only marginally to the total cooling rate. The evolution of cooling during the first 50 Myr and the onset of collapse are thus almost independent of the metallicity of the gas, at least for metallicities $Z \leq 10^{-3} Z_{\odot}$. Once gas at the center of the halo begins to collapse, however, the contribution of fine structure cooling does increase, and differences between the metal-enriched and the zero-metallicity models become more pronounced. Nevertheless, only in run L1 do we see a significant difference in the fraction of gas accumulated in the sink particle by the end of the simulation.

The influence of the UV background on the gas in these simulations remains the same

as in the zero metallicity case. Cooling and collapse is delayed or inhibited depending on the strength of the background radiation field. The metals in the gas cannot initiate collapse if the gas would not collapse without the metals present.

4. Discussion

At first sight, the fact that fine structure cooling from metals has so little impact on the thermal or dynamical evolution of the gas even when $Z = 10^{-3} Z_{\odot}$ is somewhat surprising, given that Bromm et al. (2001) found that gas with this metallicity could cool rapidly and fragment even in the absence of molecular hydrogen. However, comparison of the cooling time due to fine structure emission to the free-fall time helps to make the situation clear. The cooling time due to fine structure emission is given by

$$t_{\text{cool,fs}} = \frac{1}{\gamma - 1} \frac{n k T}{\Lambda_{\text{fs}}}, \quad (2)$$

where Λ_{fs} is the total cooling rate per unit volume due to fine structure emission, T is the temperature of the gas, γ is the adiabatic index, n is the number density of the gas and k is the Boltzmann constant. The free-fall time can be written as

$$t_{\text{ff}} = \left(\frac{3\pi}{32G\rho} \right)^{1/2}, \quad (3)$$

where G is the gravitational constant and $\rho = \rho_{\text{gas}} + \rho_{\text{dm}}$. The gas density ρ_{gas} can be written in terms of the number density n as $\rho_{\text{gas}} = \mu n$, where μ is the mean molecular weight of the gas.

In Figure 5, we indicate the temperatures and densities at which $t_{\text{cool,fs}} = t_{\text{ff}}$ for $10^{-3} Z_{\odot}$ gas, for three different assumed fractional ionizations, with $x_e = 1.0$ (fully ionized gas), $x_e = 10^{-2}$, and $x_e = 10^{-4}$. In each case, we assume that the carbon and silicon are present only as C^+ or Si^+ , since a fairly small external UV flux is sufficient to achieve this. In the $x_e = 1.0$ case, we also assume that all of the oxygen is O^+ , since charge transfer between oxygen and hydrogen, which have nearly identical ionization potentials, ensures that $x_{\text{O}^+}/x_{\text{O}} \simeq x_{\text{H}^+}/x_{\text{H}}$. For the dark matter density ρ_{dm} , we adopt the value found at the center of our model protogalactic halo at $t=0$, $\rho_{\text{dm}} \simeq 8 \times 10^{-22} \text{ g cm}^{-3}$. In the plot, regions to the left of the line have $t_{\text{cool,fs}} > t_{\text{ff}}$, while those to the right have $t_{\text{cool,fs}} < t_{\text{ff}}$.

At the beginning of our simulations, gas in the center of the halo has a temperature $T = 10^4 \text{ K}$ and a number density $n = 0.03 \text{ cm}^{-3}$. It therefore lies outside of the regime where fine structure cooling is efficient, and so it is not surprising that we find that metal-line cooling is initially unimportant. As the gas cools, whether through Compton cooling

or H_2 emission, and begins to compress as it falls in to the halo, it moves towards the temperature and density regime in which fine structure cooling is effective, as can be seen from the evolutionary trajectories plotted in Figure 5. At the same time, however, the gas is recombining, which moves the boundary of this regime to the right of the plot, towards higher densities. The physical reason for this shift is the fact that free electrons are much more effective than neutral hydrogen at exciting the C^+ and Si^+ fine structure lines, and so electron excitation dominates for $x_e > 10^{-2}\text{--}10^{-3}$, depending on the temperature. The net effect is that fine structure cooling remains of little importance until the gas is near the high-cooling regime. This only happens after considerable cooling and compression has already taken place, and therefore does not occur at all if H_2 cooling is ineffective, as in runs Z3 and L3.

Why then do Bromm et al. (2001) come to such a different conclusion? The answer lies in the difference between the initial conditions used in their simulations and in ours. The gas in their simulations has an initial temperature of 200 K at $z = 100$, and its temperature falls further due to adiabatic cooling in the IGM prior to the formation of their simulated protogalactic halo at $z \sim 30$. Since this halo has a mass of $2 \times 10^6 \text{M}_\odot$ and a virial temperature $T_{\text{vir}} \simeq 5000$ K, the temperature of the gas at the moment at which the halo forms is very much smaller than the halo virial temperature. Consequently, thermal pressure is initially unable to prevent the collapse of gas into the halo. As it collapses, the gas heats up, and the thermal pressure eventually becomes large enough to halt the collapse. However, this does not occur until the gas temperature is approximately equal to the halo virial temperature, by which time the gas density has increased to a value $n \simeq 300 \text{ cm}^{-3}$. As can be seen from Figure 5, gas with this density and with a temperature of 5000 K lies close to or within the regime where $t_{\text{cool,fs}} < t_{\text{ff}}$ (depending on its fractional ionization), and so it is not surprising that Bromm et al. (2001) find that fine structure cooling is effective and that the gas can cool even in the complete absence of H_2 .

On the other hand, in our simulations the high initial temperature of 10^4 K and lower virial temperature $T_{\text{vir}} \simeq 1900$ K mean that $T_{\text{gas}} > T_{\text{vir}}$ initially, and that thermal pressure support is important right from the start. Indeed, at the beginning of our simulations pressure precisely balances gravity, by design. Therefore, there is no initial phase of free-fall collapse as in the Bromm et al. (2001) simulations. Instead, significant gravitational contraction occurs only if the gas is able to cool to a temperature of order T_{vir} or below, which, since fine structure cooling is initially ineffective, will only occur if enough H_2 can form in the low density gas.

Therefore, the key question is which set of initial conditions is more appropriate. It is difficult to see how intergalactic gas could become metal enriched without at some point

being ionized. Previous calculations have shown that the size of a typical region enriched by a population III supernova is much smaller than the size of the H II region created by its progenitor star (see e.g. Bromm et al. 2003). We would therefore expect our initial conditions to be more appropriate than those of Bromm et al. (2001) for treating recently enriched and ionized regions. However, if enough time elapses following the enrichment event for the gas to be able to cool down to a temperature of a few hundred K, then the Bromm et al. (2001) initial conditions will be more appropriate. As Oh & Haiman (2003) show, this is most likely to occur in high redshift gas with a low overdensity. Then Compton cooling is fast and highly effective and can cool the gas to $T \sim 300$ K within a recombination time. On the other hand, at lower redshifts, or at higher overdensities, the gas recombines faster than it cools, and the temperature that can be reached by Compton cooling alone is much higher. This is the case in our simulated halos. Note that in either case the metals play no significant role in determining whether or not the gas is able to collapse.

An important implication of these results is that if we are primarily concerned with investigating questions such as how M_{crit} evolves with redshift, or how UV feedback in the form of Lyman-Werner photons affects the ability of the gas to cool, then we need not worry about the effects of metal enrichment. This is because the thermal evolution of the gas on the scales of interest for these questions is completely dominated by Compton cooling and/or H₂ cooling. Therefore, results from studies such as Haiman et al. (2000) or Yoshida et al. (2003) give a better guide to the behaviour of small, low-metallicity protogalaxies than might have been anticipated (although the additional complications posed by the mechanical energy injected into the gas by H II regions and supernovae do of course still need to be taken into account).

Finally, it is important to stress that our results do not address the question of whether or not there is a critical metallicity Z_{crit} above which fine structure cooling from metals allows efficient fragmentation to occur. This is because if fragmentation does occur, we would expect it to occur at densities $n > 500 \text{ cm}^{-3}$ which are unresolved in our current simulations. We will examine this question with much higher resolution simulations in the future.

We thank Z. Haiman and S. Kitsionas for useful discussions. R.S.K. and A.K.J. acknowledge support from the Emmy Noether Program of the Deutsche Forschungsgemeinschaft (grant no. KL1358/1). M.-M.M.L. and S.C.O.G. acknowledge support from NSF grants AST99-85392 and AST03-07793 and NASA grants NAG5-10103 and NAG5-13028. The simulations were performed on the PC cluster “sanssouci” at the Astrophysikalisches Institut Potsdam.

REFERENCES

Abel, T., Bryan, G. L., & Norman, M. L. 2002, *Science*, 295, 93

Bate, M. R., Bonnell, I. A., & Price, N. M. 1995, *MNRAS*, 277, 362

Bate, M. R. & Burkert, A. 1997, *MNRAS*, 288, 1060

Benz, W. 1990, in *Numerical Modelling of Nonlinear Stellar Pulsations Problems and Prospects*, ed. J. R. Buchler (Dordrecht: Kluwer), 269

Black, J. H. & Dalgarno, A. 1977, *ApJS*, 34, 405

Bromm, V., Coppi, P. S., & Larson, R. B. 2002, *ApJ*, 564, 23

Bromm, V., Ferrara, A., Coppi, P. S., & Larson, R. B. 2001, *MNRAS*, 328, 969

Bromm, V. & Larson, R. B. 2004, *ARA&A*, 42, 79

Bromm, V., Yoshida, N., Hernquist, L. 2003, *ApJ*, 596, L135

Burton, M. G., Hollenbach, D. J., & Tielens, A. G. G. M. 1990, *ApJ*, 365, 620

Cen, R. 1992, *ApJS*, 78, 341

Ciardi, B. & Ferrara, A. 2005, *Space Sci. Rev.*, 116, 625

Cojazzi, P., Bressan, A., Lucchin, F., Pantano, O., & Chavez, M. 2000, *MNRAS*, 315, L51

Glover, S. C. O. 2005, *Space Sci. Rev.*, 117, 445

Glover, S. C. O., 2006, in preparation.

Glover, S. C. O. & Brand, P. W. J. L. 2001, *MNRAS*, 321, 385

Glover, S. C. O. & Brand, P. W. J. L. 2003, *MNRAS*, 340, 210

Glover, S. C. O., Savin, D. W., & Jappsen, A.-K. 2005, *ApJ*, submitted; astro-ph/0506221

Haiman, Z., Abel, T., & Rees, M. J. 2000, *ApJ*, 534, 11

Jappsen, A.-K., Glover, S. C. O., Klessen, R. S., & Mac Low, M.-M. 2006, in preparation

Jappsen, A.-K., Klessen, R. S., Larson, R. B., Li, Y., & Mac Low, M.-M. 2005, *A&A*, 435, 611

Kogut, A., Spergel, D. N., Barnes, C., et al. 2003, *ApJS*, 148, 161

Le Bourlot, J., Pineau des Forêts, G., & Flower, D. R. 1999, MNRAS, 305, 802

Machacek, M. E., Bryan, G. L., & Abel, T. 2001, ApJ, 548, 509

—. 2003, MNRAS, 338, 273

Mashchenko, S., Couchman, H. M. P., & Sills, A. 2005, ApJ, accepted; astro-ph/0511361

Matsuda, T., Satō, H., & Takeda, H. 1969, Progress of Theoretical Physics, 42, 219

Monaghan, J. J. 1992, ARA&A, 30, 543

Navarro, J. F., Frenk, C. S., & White, S. D. M. 1997, ApJ, 490, 493

Oh, S. P. & Haiman, Z. 2003, MNRAS, 346, 456

Omukai, K., Tsuribe, T., Schneider, R., Ferrara, A., 2005, ApJ, 626, 627

Peebles, P. J. E. & Dicke, R. H. 1968, ApJ, 154, 891

Pettini, M. 1999, in Walsh J. R., Rosa M. R., eds, ESO Astrophys. Symp., Chemical Evolution from Zero to High Redshift. Springer, Berlin, p. 233

Ricotti, M., Gnedin, N. Y., & Shull, J. M. 2002, ApJ, 575, 33

Ricotti, M., Ostriker, J. P., 2004, MNRAS, 350, 539

Saslaw, W. C. & Zipoy, D. 1967, Nature, 216, 976

Spergel, D. N., Verde, L., Peiris, H. V., et al. 2003, ApJS, 148, 175

Springel, V., Yoshida, N., & White, S. D. M. 2001, New Astronomy, 6, 79

Tegmark, M., Silk, J., Rees, M. J., et al. 1997, ApJ, 474, 1

Yoshida, N., Abel, T., Hernquist, L., & Sugiyama, N. 2003, ApJ, 592, 645

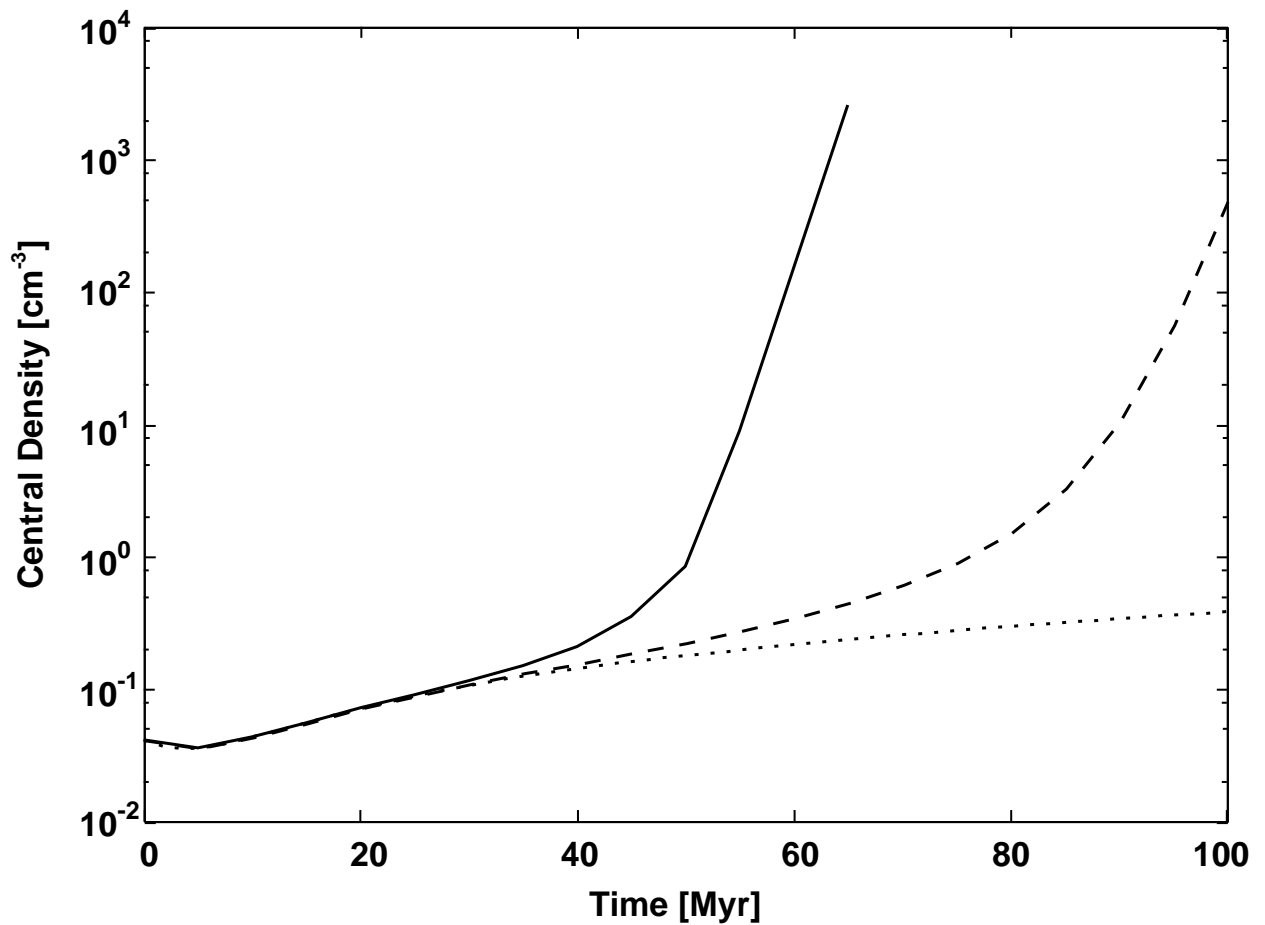


Fig. 1.— The time evolution of the gas density within the scale radius r_s of the dark-matter potential. We show runs Z1 (*solid line*), Z2 (*dashed line*) and Z3 (*dotted line*) which all have zero metallicity. The UV background increases from run Z1 to run Z3 (see Table 1). For clarity, we only plot the evolution up until the point at which a sink particle forms (or until the end of the run, if no sink forms).

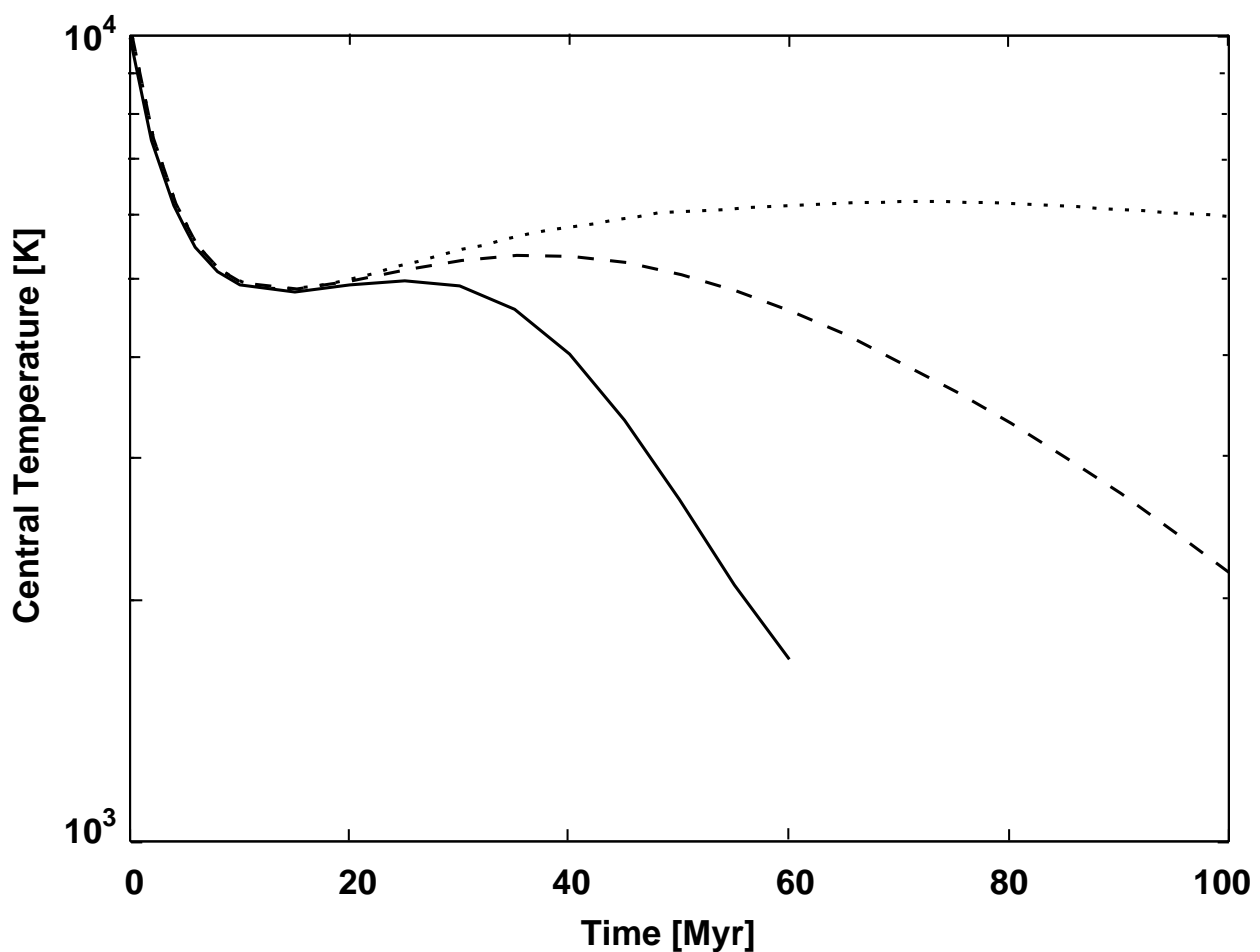


Fig. 2.— Same as Figure 1, but for the central temperature of the gas.

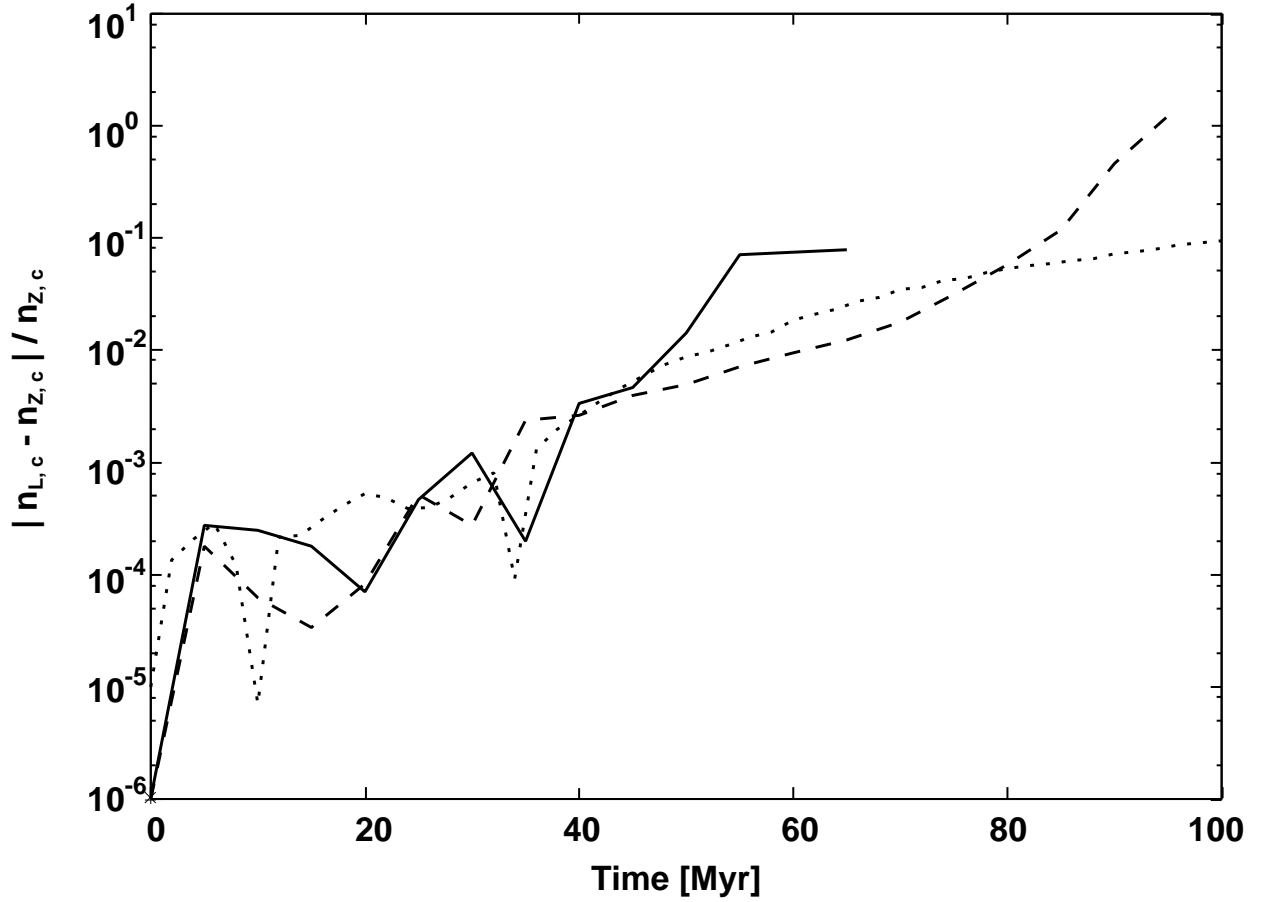


Fig. 3.— The time evolution of the relative difference $|n_{Z,c} - n_{L,c}|/n_{Z,c}$, where $n_{L,c}$ is the central gas density in the runs with low-metallicity gas and $n_{Z,c}$ the central gas density in the runs with zero-metallicity gas. We show the values for runs L1 (solid line), L2 (dashed line) and L3 (dotted line) compared to the Z runs with the same UV background. The UV background increases from run L1 to run L3 (see Table 1). For clarity, we only plot the evolution until the point at which a sink particle forms (or until the end of the run, if no sink forms).

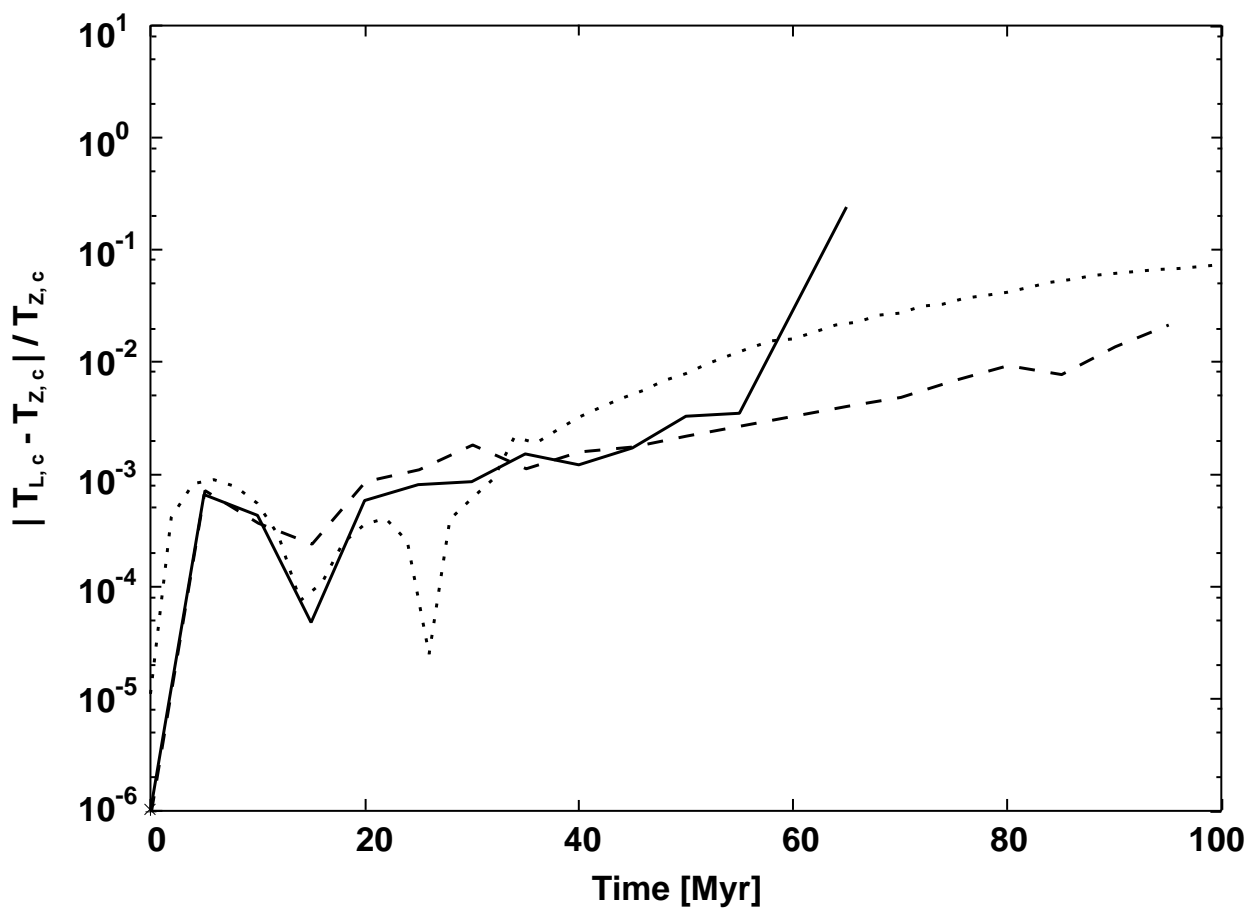


Fig. 4.— Same as Figure 3, but for the central temperature of the gas.

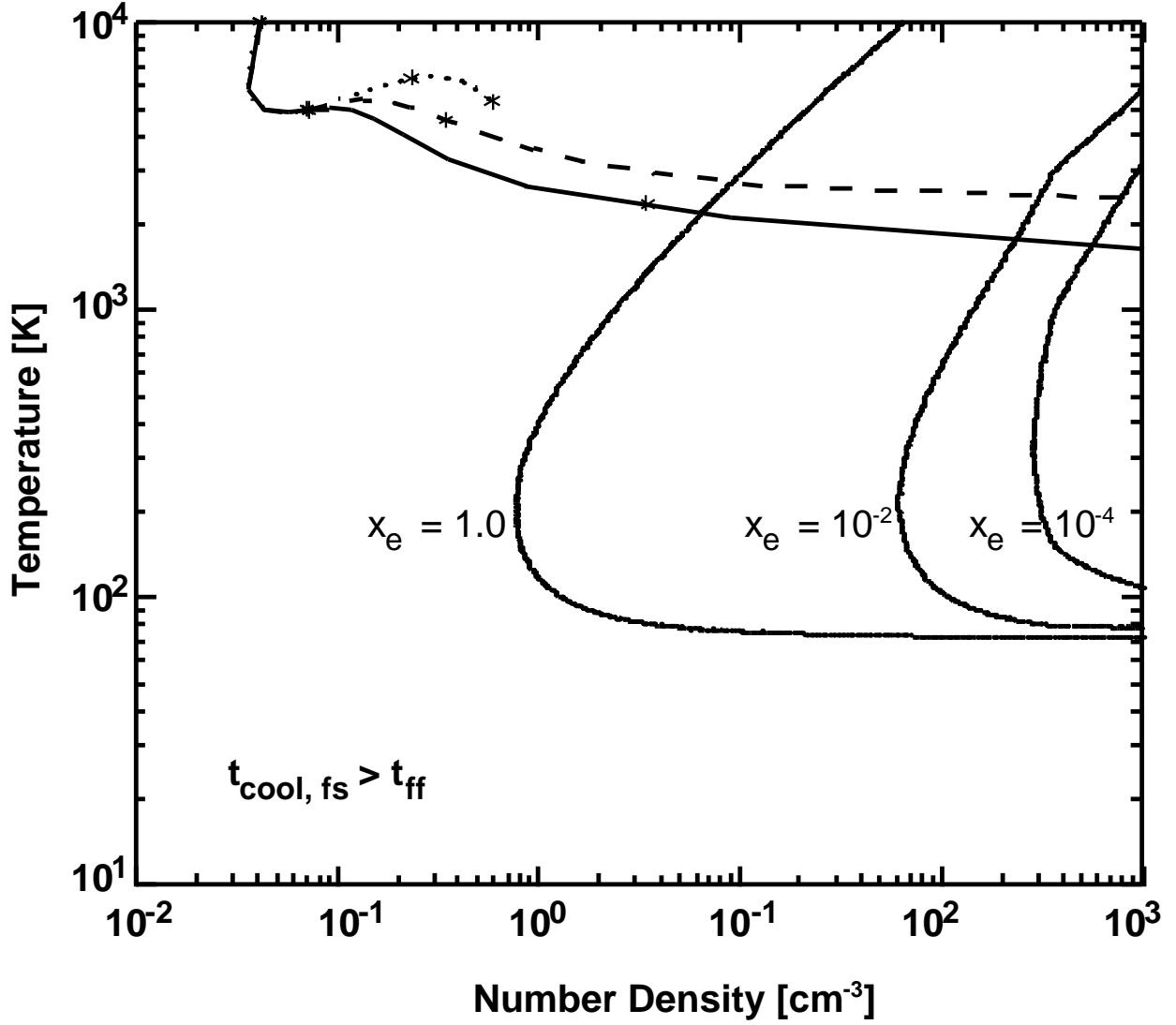


Fig. 5.— The solid contours indicate the temperature and density at which the cooling time due to fine structure emission, $t_{\text{cool,fs}}$, equals the free-fall time, t_{ff} , for gas with a metallicity $Z = 10^{-3} Z_{\odot}$ and with fractional ionizations $x_e = 1.0$, $x_e = 10^{-2}$ and $x_e = 10^{-4}$. To the left of each line, $t_{\text{cool,fs}} > t_{\text{ff}}$, so metal cooling is inefficient. In every case, we assume that all of the carbon and silicon is present as C^+ and Si^+ respectively. In the $x_e = 1.0$ case, we assume that all of the oxygen is present in the form of O^+ , but otherwise that it is all $\text{O}1$. To compute the free-fall time, we take the density to be the sum of the gas density ρ_g and the dark matter density at the center of the halo ρ_{dm} . The figure also shows how the temperature and density of the gas at the centre of the halo evolve in runs L1 (*solid line*), L2 (*dashed line*) and L3 (*dotted line*). The evolution of the fractional ionization in these runs is indicated by the star symbols: $x_e = 1.0$ for $T = 10^4$ K, and decreases by a factor of 10 between each successive star.

Table 1. Physical state of the densest gas within the scale radius r_s after 100 Myr

Run	Z^a (Z_\odot)	J_{21}^b	$T_{c,\min}^c$ (K)	$n_{c,\max}^d$ (cm^{-3})	$x_{\text{H}_2,c,\max}^e$	f_{sink}^f
Z1	0.0	0.0	< 200	> 500	4×10^{-3}	0.17
L1	10^{-3}	0.0	< 200	> 500	2×10^{-3}	0.20
Z2	0.0	10^{-2}	< 200	> 500	5×10^{-4}	0.005
L2	10^{-3}	10^{-2}	< 200	> 500	5×10^{-4}	0.01
Z3	0.0	10^{-1}	4400	0.7	1.6×10^{-5}	0.0
L3	10^{-3}	10^{-1}	5900	0.6	1.5×10^{-5}	0.0

^aMetallicity of the gas.

^bStrength of the UV background.

^cMinimum temperature of the gas within the scale radius r_s .

^dMaximum number density of the gas within the scale radius r_s .

^eMaximum fractional H_2 abundance within the scale radius r_s .

^fMass fraction of gas within a sink particle.